

SPINNER SHED ICE ENGINE INGESTION ASSESSMENT METHODOLOGY

Luis P. Ruiz-Calavera*, **Sergio Cid-Arroyo****, **Luis Benitez-Montañes*****
***Flight Physics CoC, **Aerodynamics Domain, ***Structural Dynamics Domain**
Airbus Defense and Space, Getafe, Spain

Keywords: *turboprop, ice, ingestion*

Abstract

A simplified methodology based on a combination of theoretical/numerical analysis and ground tests has been developed to evaluate the probability that ice shed from the spinner of a turboprop is ingested by the engine. This methodology has been used to support the A400M demonstration of compliance with the certification requirement that accumulation of ice on the spinner does not affect engine operation. This paper presents the details of the methodology.

1 Introduction

One of the many elements that need to be taken into account during a turboprop aircraft certification process is that of ice ingestion by the engines. In particular it is needed to demonstrate [1] that no ice accreted on the aircraft, if shed and ingested by the engine, will produce an unacceptable damage to the engine or a serious power loss (EASA CS 25.1093: Air intake system de-icing and anti-icing provisions). Bench tests are performed with the engine to characterize the engine ice ingestion capability at various powers and temperature levels (e.g. the ice slab ingestion test of AC20-147 [2] to demonstrate compliance with FAR 33.77 [3]) out of which the allowed budget for ice ingestion is known. The next step is then to demonstrate that the pieces of ice reaching the engine, if any, do not exceed the acceptable limit.

For turboprops, the sources of possible ice ingestion are typically the ice accumulated on the spinner, the propeller blades and the engine intake. The latter two are normally either de-

iced or anti-iced, so that there are limits to the maximum amount of ice that can accumulate and consequently shed from them. On the other hand, spinners may or may not be protected from ice depending on necessity. For the A400M military transport aircraft (Fig. 1) it was decided not to protect the spinner to reduce system complexity and energy consumption. Therefore it was necessary to demonstrate that as a consequence of ice accretion on the spinner no ice piece larger than a certain mass would reach the engine (Figure 2)



Fig. 1. Airbus A400M Military Transport

A tool was needed to estimate the probability of spinner ice ingestion by the engine, both during the development phase to support the decision not to protect the spinner, and during the certification phase to support the overall case put in front of the airworthiness authority to show compliance with CS 25.1093. A new methodology using a combination of theoretical and numerical analysis, ground tests and limited flight testing was used for this purpose. Demonstration only by flight test would have been more difficult and costly due to the complication of finding the right

atmospheric conditions for natural ice accretion, and especially because the process of ice shedding and subsequent engine ingestion has inherent random elements, so that the number of flights needed for the full demonstration would have been prohibitory high.

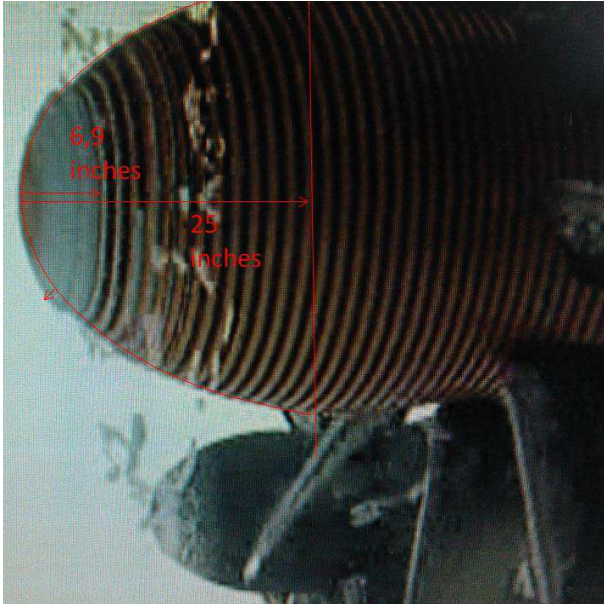


Fig. 2. Spinner Ice Shedding

Given the large number of parameters and conditions to be considered, a large number of simulations were envisaged, so one of the requirements to the tool developers was that its computational cost should not be too high. This paper presents the details of the methodology.

2 Overview of the methodology

The objective is to calculate the probability that the engine ingests ice pieces of a mass (m_{ice}) equal or greater than that which the engine can accept. This probability is built up by the following terms:

1) The probability (P_1) that ice of mass m_{ice} detach from the spinner. Given the complex physical phenomena affecting the shedding of ice (temperature, vibrations, aerodynamic pressures and shear stress, changes in centrifugal forces due to throttle variations, etc.) the conservative assumption is made that if it is possible to accumulate on the spinner a mass of ice equal or greater than m_{ice} then it is possible that it will detach, and thus $P_1=1$.

2) The probability (P_2) that the trajectory of the ice slab or sheet brings it inside the intake.

3) The probability (P_3) that if the trajectory of the ice slab or sheet is such that it would enter the intake, the ice is able to cross the propeller without being struck by the blades.

4) The probability (P_4) that, once the ice piece has reached the intake, it is effectively ingested by the engine and it is not captured by the Inertial Particle Separator (IPS).

To calculate the previous probabilities the following elements are needed:

1) Calculation of the ice shapes that can accumulate on the spinner using an ice accretion simulation code.

2) Calculation of the flow field around the front part of the nacelle and inside the intake duct using a CFD model.

3) Calculation of the trajectories followed by ice slabs or sheets shed from the spinner with a defined size and mass, to determine the probability that they enter the intake. This is done using a Monte-Carlo approach.

4) Calculation of the probability that ice slabs or sheets of a defined size are able to cross the propeller not being smashed by the propeller blades. This is done by means of a kinematic model.

5) For the ice sizes and masses with a non-negligible probability to reach the intake after crossing the propeller, it is needed a model of the behavior of the ice piece as it hits the engine intake surface. For this purpose a laboratory test was performed using an ice impact test facility. These tests allowed to characterize the fracture mechanics of the ice slabs, and in particular provided information about whether the ice slabs rebound or are smashed.

6) Calculate whether after impact the ice pieces are captured by the inertial particle separator in the intake or on the contrary they are ingested by the engine. This study is performed using a CFD analysis.

Following are the details of each of these elements.

3 Ice Shapes

The ice shapes on the spinner were calculated by the A400M propeller manufacturer RFHS (Ratier-Figeac / Hamilton-Sundstrand) using the NASA Lewice ice

accretion code. For the present analysis three different ice shapes were considered:

1) The ice shape corresponding to the largest ice accretion condition, which for this particular spinner corresponds to a 45 minutes holding in CS25 Appendix C continuous maximum icing conditions. This is the blue line in Figure 3, where it can be seen that it corresponds to a glaze ice type.

2) The ice shape corresponding to the same flight condition than the previous one but at lower temperature so that a rime ice type results. This is the red line in Figure 3. This shape is considered because it accumulates ice in a different area of the spinner and this has an influence on the trajectory of the detached ice.

3) During flight tests it was observed ice shedding of two different types. One sort is driven mainly by centrifugal forces and/or vibrations and occurs during regular build/shed cycles (Figure 2). The second type is driven by the ice/spinner bonding being weakened by the increase of ambient temperature and occurs after partial melting of the ice shape typically resulting in a release of a large part (or all) of the remaining ice shape. The two previous shapes are adequate to cover the first type of shedding mechanism. To cover the second type an additional ice shape has been defined to represent an intermediate stage during the melting process. This is the green curve in Figure 3. The shape has been selected based on the experience accumulated during the flight tests.

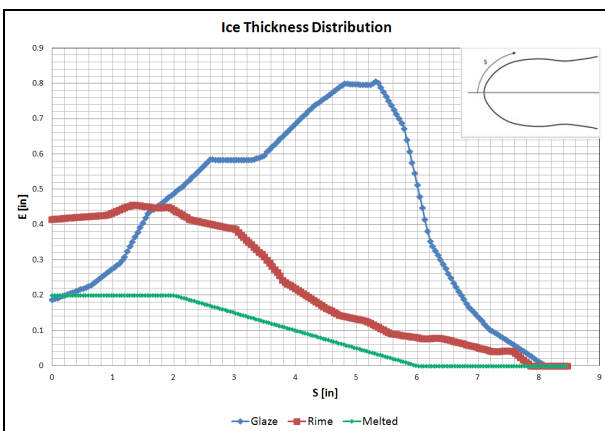


Fig. 3. Ice shapes thickness distributions

4 CFD Model

The local flow velocities around the nacelle and inside the engine intake and IPS are calculated using a CFD model of the front part of the A400M nacelle including the propeller, as shown in Figure 4.

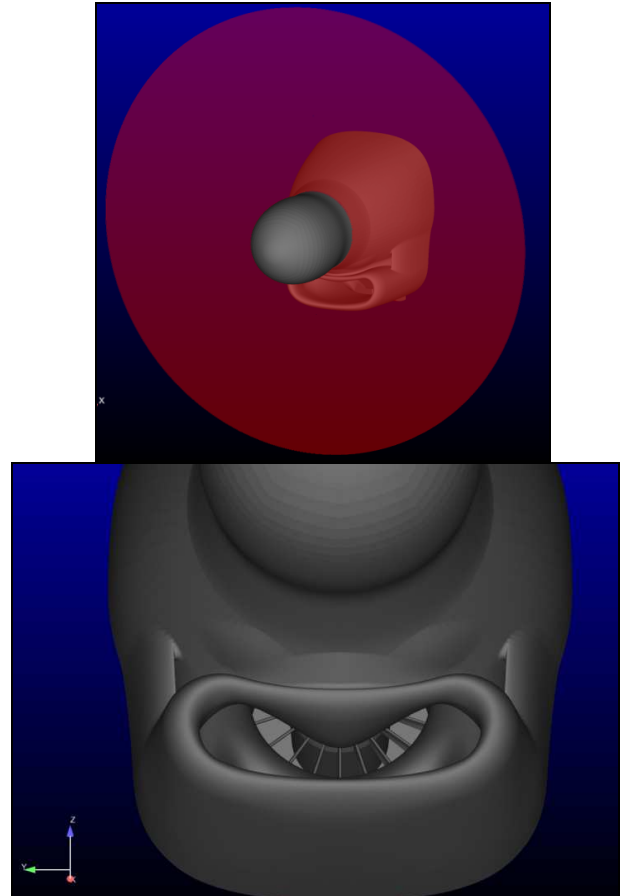


Fig. 4. CFD model geometry

To take into account the interference effects from the aircraft onto the flow-field around the nacelle the complete aircraft geometry should have been modelled, but this would have resulted in very lengthy and costly calculations. The following procedure was used instead:

1) For the desired flight condition identified by the flight velocity, the altitude, the ambient temperature, the A/C weight, and the engine power, the corresponding values of propeller rotational speed, blade pitch angle, propeller thrust and engine mass flow are calculated with the engine deck, and the A/C angle of attack is determined from the aircraft performance deck.

2) The local angle of attack and the local angle of sideslip of the isolated nacelle for the CFD calculations are approximated by the inflow angles of the installed propeller corresponding to the aircraft and engine operating conditions under consideration obtained from the aircraft 1P loads aerodynamic database.

In this way all the boundary conditions needed for the CFD calculations are known, including the required mass flows through the engine inlet and the IPS.

Using this working method a simple mesh of only $5 \cdot 10^6$ elements can be used to generate the required flow fields resulting in very quick convergence times. Figure 5 shows a cut through the center plane of the mesh.

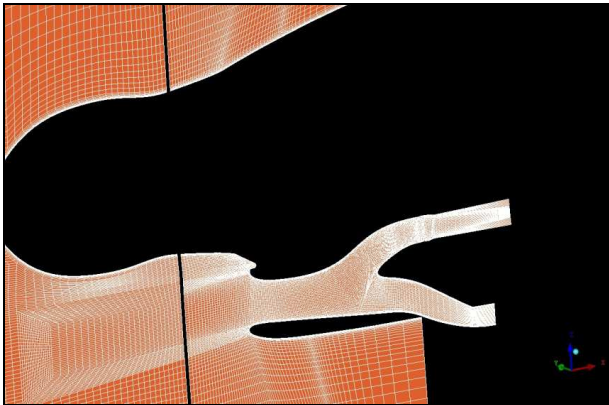


Fig. 5. CFD grid

The propeller is modelled using a VBM (Virtual Blade element Model) which takes into account the propeller geometry and aerofoils aerodynamic data, its pitch angle and rotational speed. Figure 6 shows an example of the distribution of the x-component of the flow speed on both the centre plane of the nacelle and on a plane located 20cm in front of the propeller (and thus in the spinner region) for a go-around condition at maximum take-off power. The propeller effect, including the interaction with the angle of attack can be clearly seen.

All RANS calculations have been performed using the $k-\omega$ SST turbulence model. Once the CFD calculation is converged, the resulting velocity fields are interpolated into a cartesian mesh to facilitate its use during the ice trajectory calculations.

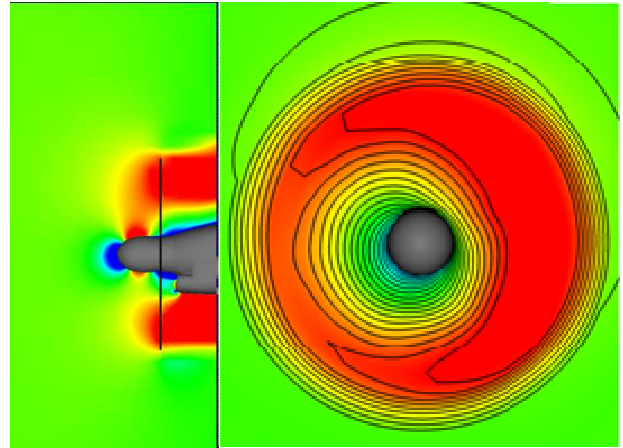


Fig. 6. Propeller flow pattern

4 Ice slabs trajectory calculation

The trajectory of an ice slab is simulated using a 3-DOF (Degrees of Freedom) analysis, that is to say, only the position of its center of gravity is calculated but not its attitude angles. Furthermore, in terms of aerodynamic forces, only the drag is considered, that is, the effect of lift and/or side-force on the ice slab is neglected.

This simplification is necessary as the ice slabs can have very different shapes and thus it is not economically realistic to obtain a full aerodynamic data base for each of them. Nevertheless the approximation is acceptable given the fact that the trajectory to reach the inlet from the spinner is very short (approximately 1.7m). To cover different ice shapes and to compensate for the lack of lift and side force, a wide range of drag coefficients (see below) are considered to produce a large scatter of the trajectories.

The kinematic of the ice is initially constrained due to the fact that it is on the spinner surface so that components of velocity and acceleration in the inward direction of the normal vector of the spinner surface at the contact point are eliminated. Once the ice has left the surface of the spinner the previous constraint disappears and the acceleration of the ice in the nacelle reference frame is simply:

$$\vec{a} = \vec{g} + \varphi \cdot V_R^2 \frac{\vec{V}_R}{|V_R|} \quad (1)$$

where g is the acceleration of gravity V_R is the relative velocity between the ice and the local flow velocity and φ is the ballistic coefficient, that for a flat slab or sheet of ice only depends

on the ice thickness e , the drag coefficient C_d , and the relative densities of air and ice.

$$\varphi = \frac{\rho_{air} \cdot C_d}{2 \cdot \rho_{ice} \cdot e} \quad (2)$$

The initial conditions correspond to the ice piece located on the spinner at a particular position with the circumferential velocity resulting from the spinner angular velocity, and zero axial and radial velocity components relative to the nacelle.

For each flight condition to be studied, for each accreted ice shape being considered, and for each desired combination of ice mass, size and density (out of which the ice slab/sheet thickness e can be derived) a Monte-Carlo analysis is performed with the following statistical variables:

1) Initial longitudinal position of the ice piece along the spinner. It has to be taken into account that for a given accreted ice shape (glace, rime, or melt) a slab/sheet of thickness e can only detach from the range of positions in Figure 3 where the ice accretion thickness is equal or larger than e . Within this region the initial position is generated using a statistically uniform distribution.

2) Initial circumferential position of the ice piece around the spinner. Determined from a statistically uniform distribution between 0° and 360°

3) Drag coefficient of the ice piece. Determined from a statistically uniform distribution between 0.4 and 1.4

Typically roughly 100.000 Monte-Carlo simulations are done for each combination of flight condition, accreted ice shape, ice mass, density and size. Figure 7 shows an example of the Monte-Carlo trajectories. The trajectories that reach the intake inlet (Figure 8) are tracked with three different purposes:

1) To determine the positions and velocity of the ice piece at the time it crossed the propeller plane. This information is used for the propeller crossing modulus in the next chapter.

2) To determine the impact velocity and incidence angle to the intake duct (Figure 9). This information is used for the ice impact tests described in chapter 7.

3) To calculate the probability that the ice piece enters the intake (P_2). Figure 10 shows an example of the convergence of the results for P_2 with the number of Monte-Carlo simulations.

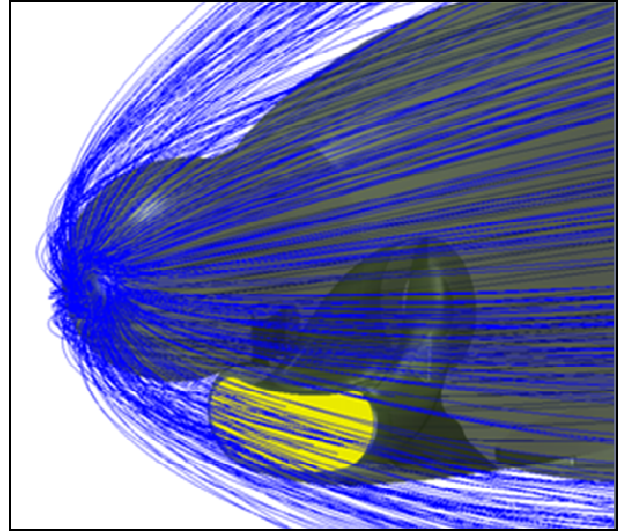


Fig. 7. Example of a Monte-Carlo simulation

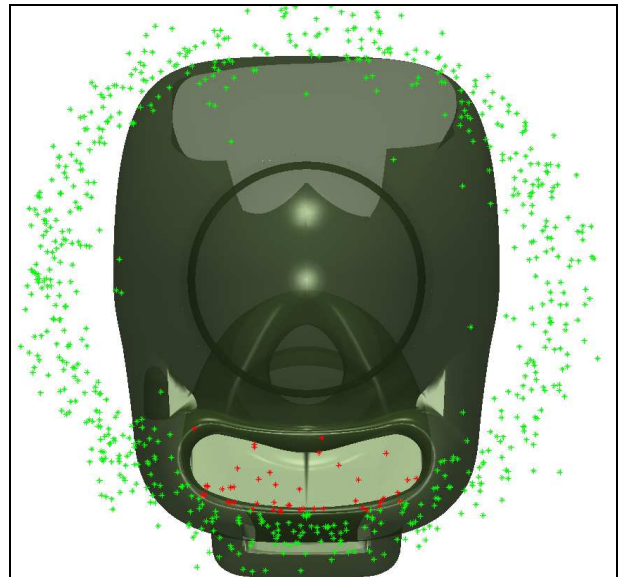


Fig. 8. Trajectories entering (red dot) and not entering (green dot) the intake. Control at intake inlet

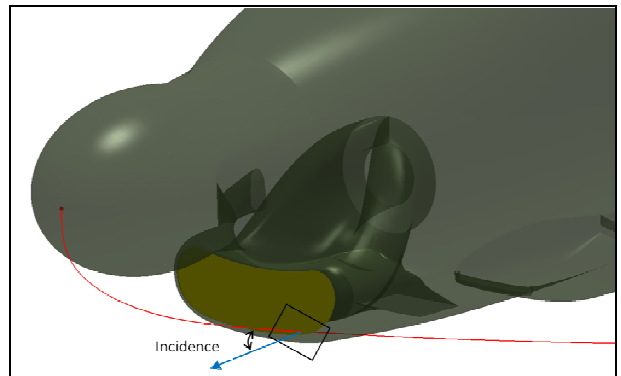


Fig. 9. Calculation of the velocity and incidence angle of the ice piece at the intake

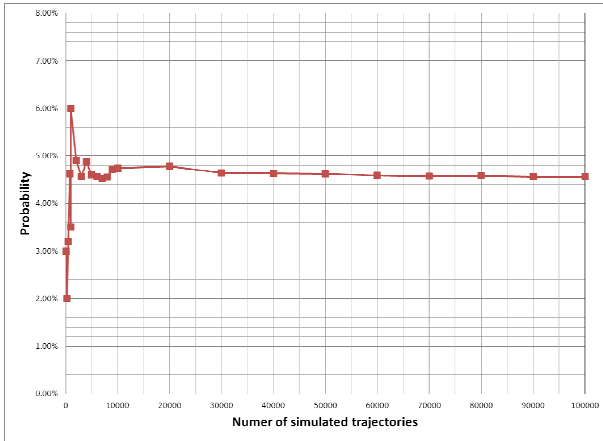


Fig. 10. P_2 probability vs. number of trajectories

5 Propeller crossing probability

The probability that an ice slab/sheet crosses the propeller without being hit by the blades is calculated by means of a simplified methodology proposed by the propeller manufacturer RFHS. The calculation compares the time that it takes for the mass of ice to pass through the blade row to the time it takes for one blade passage (see the sketch in Figure 11).

The values of the positions and velocities at which the ice slabs that enter the intake cross the propeller plane are known from the Monte-Carlo simulation performed in the previous step.

From the crossing radial position, the local blade chord and pitch angle (β) are known and can be used to decompose the blade chord in its axial (C_a) and tangential (C_t) components.

The axial distance that the ice slab needs to travel to cross the propeller is the sum of the axial chord and the axial length of the ice slab (d_a). The axial component of the relative velocity of the ice slab to the propeller is used to derive the axial time.

The circumferential distance is the blade gap G (circumferential perimeter at the crossing position divided by the number of blades) plus the tangential chord minus the tangential length of the ice slab (d_t). The relative velocity of the ice slab to the blade is the angular velocity at the local radius ($\omega \wedge r$) minus the circumferential component of the ice slab velocity relative to the propeller. The resulting velocity is used to derive the circumferential time.

Initially it is assumed that the ice slab enters the blade row just after the blade leading

edge has passed. This produces the longest possible circumferential time. If the axial time is less than the circumferential time, then it is possible for the ice slab to traverse the propeller. To assign a probability (P_3) the excess time (circumferential time minus axial time) is compared to the blade passing time in order to account for the possibility of the ice slab entering the passage at other than the optimal time.

To cover the fact that the trajectory simulation does not monitor the space orientation of the ice slab the following procedure is followed. The assumption is made that the ice slab is a rectangular shaped parallelepiped of constant thickness. The axial and circumferential times are calculated for the six possible combinations of length, width, and thickness of the ice slab to take into account the different possible orientations of the ice slab at the time it crosses the propeller. The probability is then taken as the average of these partial probabilities.

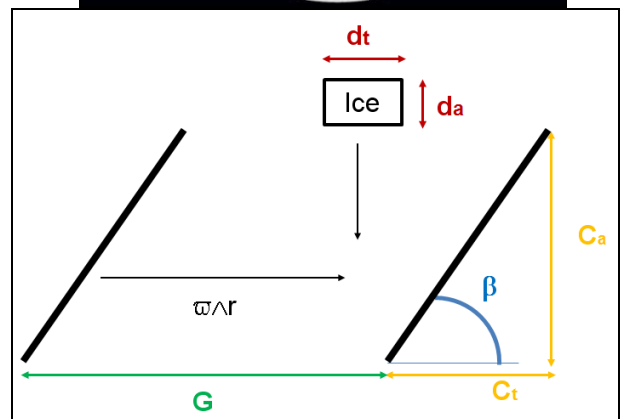
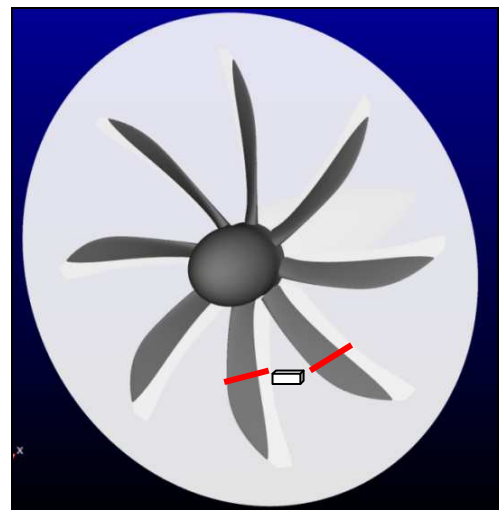


Fig. 11. Propeller crossing sketch

6 Results

The previously described methodology has been used to calculate the probability of intake ingestion for different flight conditions, for both inboards and outboard engine, and for different combinations of ice piece sizes, masses and densities. A systematic analysis of all possible combinations needs to be performed as it is not possible to determine a-priori which is the worst condition. In general the probability that ice piece trajectories go into the intake increases for intermediate flight speeds, for lower ice densities and for smaller ice thicknesses as all of these elements increase the ratio of aerodynamic forces to inertia forces on the ice piece (if the aerodynamic forces on the piece of ice are small the motion is dominated by the initial angular velocity associated to the spinner rotation and the trajectory is roughly contained in a vertical plane; on the contrary, for very high flight speeds, the trajectory is basically straight backwards with no intersection with the inlet). Higher local angles of attack (due to flying at higher weight, lower speeds or to the use of flaps) tend to also increase the probability, as the flow incoming from the bottom side of the spinner tends to push the ice pieces towards the inlet. In the same way higher engine powers increase the mass flow through the intake and thus the probability that it captures the ice slab.

Concerning the probability to cross the propeller the situation is different. Higher aerodynamic forces will result in higher crossing velocities which will increase the crossing probability, but, on the other hand, they will also reduce the crossing radial position, which reduces the blades gap and thus the probability of crossing. Obviously larger ice slabs have less probability of crossing than smaller ones.

For the A400M the highest ingestion probability that was found corresponded to a final approach flight phase at VLS for 20° flaps, engines power setting to flight idle, very cold atmosphere (ISA -45°) at sea level altitudes with a 150gr ice slab of 800Kg/m³ density and a thickness of 0.2 inches (area of 57 inch²) detaching from the glaze ice shape of Figure 3 on the outboards engine.

For this combination of parameters the probability that the trajectories were directed towards the intake was of $P_2=4\%$. Out of those trajectories $P_3=2.8\%$ would be able to cross the propeller, resulting in an overall intake ingestion probability of $P_2 \cdot P_3=0.1\%$.

As the probability to enter the intake is not zero it is necessary to assess the probability that once the ice slabs enter the intake they are indeed ingested by the engine.

7 Ice impact laboratory tests

The geometry of the A400M intake, with no direct line of sight from the spinner to the engine face (Figure 12), makes it impossible for an ice slab to reach the engine without previously hitting the intake duct internal walls. Furthermore, the trajectories of the Monte-Carlo analysis show that all the impacts take place on the lower part of the duct at a defined range of impact speeds (roughly between 25 and 45 m/s) and incidences (roughly between 10° and 20°).

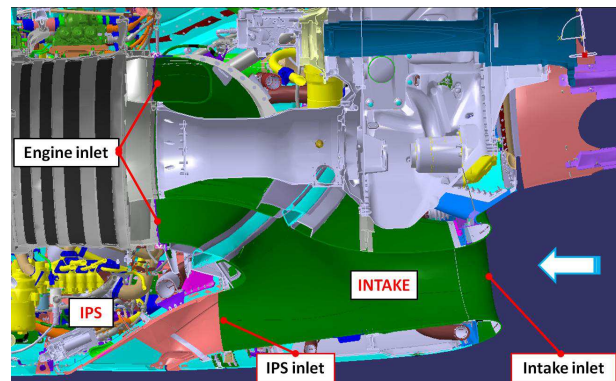


Fig. 12. A400M intake

The behavior of the ice slabs after impact is difficult to predict analytically as it will depend on the elastic properties of the intake material and the mechanical properties and shape of the ice. Several possibilities exist:

- The ice bounces fully or partially elastically and it remains in a single piece.
- The ice bounces fully or partially elastically breaking up in smaller pieces.
- The ice does not bounce because its kinetic energy is dissipated by ice and/or intake deformations and the ice remains in a single piece.
- The ice does not bounce because its kinetic energy is dissipated by ice and/or intake

deformations and the ice breaks in smaller pieces.

To clarify this issue an ice impact laboratory test has been performed using an ice cannon installed at the Carlos III University in Leganes (Madrid). This gun uses compressed air up to 2 bars to provide the low acceleration needed to shoot the ice samples without fracturing them and nevertheless reaching velocities up to 200 m/s. The ice slabs impacted on a 1.6mm thick 820x640 mm² flat plate of Aluminum 2024-T3 which has similar mechanical properties as the A400M engine air intake. This plate is supported by a steel rig frame that allows changing its incidence with respect to the incoming ice slab. A high-speed camera (8000 frames per second) is used to record the impacting sequences. Figure 13 and 14 show a sketch of the facility and a photograph of the test area.

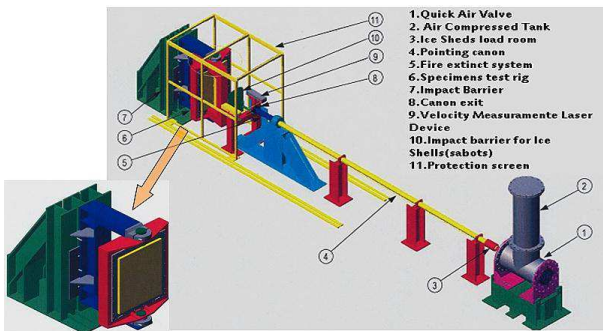


Fig. 13. Ice impact tests gun



Fig. 14. Ice impact tests gun

Silicon resin molds are used for preparing the ice-slabs in a laboratory refrigerator. To prepare a monolithic ice the mold is maintained during 24 hours at a temperature of -25 °C. Sabots made of polyurethane foam sockets envelope the ice slab when it is introduced in the gun barrel (Figure 15). Once outside of the gun after launch these sabots separate from the ice slab due to aerodynamic drag and they are stopped so that they do not interfere with the measurement and video devices.

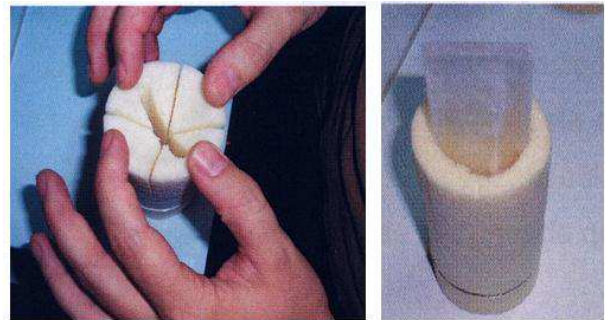


Fig. 15. Ice slab and sabot

Notwithstanding the reduced range of impact speeds and incidences necessary for spinner ice evaluation the tests have covered ice masses between 50 and 200gr, velocities between 20 and 60 m/s and incidences between 10° and 45° to enlarge the data base for possible future applications.

It is not the purpose of this paper to go into the many results obtained during these tests neither on the details of the fracture mechanics for the different combinations of ice masses, impact velocities and incidences. The quick summary is that for the range of interest for the purpose of this investigation the ice slabs are either smashed or broken with the remains sliding along the surface of the plate with no bouncing. Figure 16 shows the sequence of a typical test. Note that the ice slab image is duplicated due to the reflection on the aluminum sheet.

Transposing these results to the A400M intake, and taking into account that, as explained above, the Monte Carlo results have shown that the ice slabs always impact on the bottom part of the intake duct, the consequence is that after impact the remains of the ice slab will slide along the surface of the duct being directed towards the IPS thus exiting the intake

without being ingested by the engine. This is further supported by the fact that, as the CFD analysis shows, the air flow ingested by the engine is confined to the mid and upper part of the inlet duct, so that there is no chance that it can capture the pieces of ice resulting from the impact.

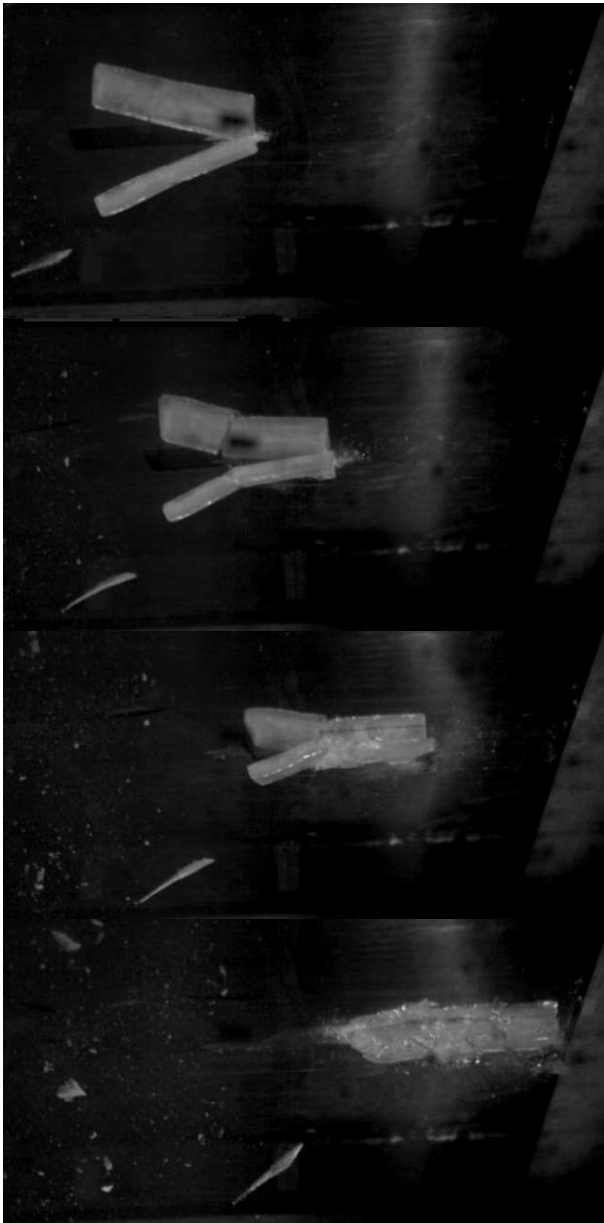


Fig. 16. Ice impact test (30m/s – 15° - 50gr)

Figure 17 shows as an example the flow pattern corresponding to final approach case identified as the one with the highest ice ingestion probability in Chapter 6. The green streamlines correspond to the air leaving through the IPS, whereas the white streamlines correspond to

those ingested by the engine. The separation between the two is readily apparent.

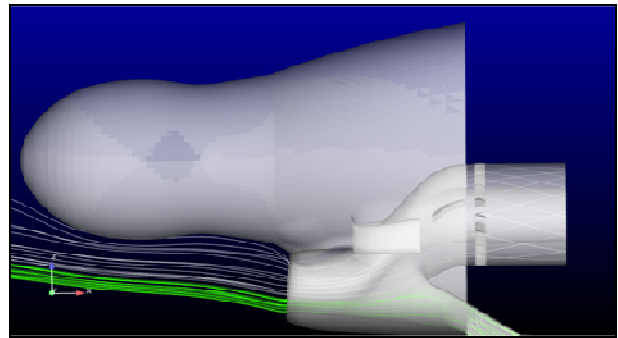


Fig. 17. Flow through the intake

8 Conclusions

A simplified methodology has been prepared using a combination of theoretical and numerical models and ground tests to evaluate the probability that ice shed from the spinner of a turboprop with a mass above that which the engine can accept is ingested by the engine. This methodology has been used both to assess the need to include a spinner anti-ice system for the A400M and, in combination with a limited number of flight tests, to demonstrate the compliance with the certification requirements that accumulation of ice on the spinner will not affect engine operation or cause a serious loss of power or thrust.

References

- [1] EASA; Certification Specifications for Large Aeroplanes; CS-25
- [2] FAA; Turbojet, Turboprop, and Turbofan Engine Induction System Icing and Ice Ingestion; AC20-147
- [3] FAA;PART 33-Airworthiness Standards: Aircraft Engines.

Acknowledgment

The authors would like to acknowledge the help of D. Perdonés-Díaz and G.C. Gallego-Cañizares from the Aerodynamics Domain of Airbus Defense and Space for their help in performing the here shown CFD calculations, and of D. Varas and J.A. Rodríguez from Carlos III University for their support during the ice impact tests. Finally a special recognition is due to Henry S. Healy and Chad Henze from Hamilton Sundstrand for their collaboration performing the spinner ice shapes calculation

and proposing the propeller passing probability calculation methodology.

Copyright Statement

The authors confirm that they, and/or their company or organization, hold copyright on all of the original material included in this paper. The authors also confirm that they have obtained permission, from the copyright holder of any third party material included in this paper, to publish it as part of their paper. The authors confirm that they give permission, or have obtained permission from the copyright holder of this paper, for the publication and distribution of this paper as part of the ICAS 2014 proceedings or as individual off-prints from the proceedings.